ELSEVIER

Aerosol Science 35 (2004) 1105–1118

Journal of
Aerosol Science

www.elsevier.com/locate/jaerosci

Theoretical and experimental study of an axial flow cyclone for fine particle removal in vacuum conditions

Chuen-Jinn Tsai[a,*], Daren-Ren Chen[b], HungMin Chein[c], Sheng-Chieh Chen[a], Jian-Lun Roth[a], Yu-Du Hsu[c], Weiling Li[b], Pratim Biswas[b]

[a] *Institute of Environmental Engineering, National Chiao Tung University, No. 75, Poai St., Hsin Chu 300, Taiwan*
[b] *Environmental Engineering Science, University of Washington in St Louis, One Brookings Dr., St Louis, MO 63130, USA*
[c] *Industrial Technology Research Institute, Center for Environmental, Safety and Health Technology Development, Chutung, Hsin Chu 310, Taiwan*

Received 17 November 2003; accepted 19 March 2004

Abstract

An axial flow cyclone to remove fine particles at low pressure conditions (6–23 torr) was designed and tested. The inner diameter of the cyclone is 3.0 cm and tested flow rates are 0.455 and 1.0 slpm. A theoretical evaluation was first carried out to calculate the particle collection efficiency and cutoff diameter for the axial flow cyclone. Experiments were then conducted to test the theory at different flow rates, pressures and cyclone designs. It was demonstrated that at sufficiently low pressure of 6 torr (flow rate = 0.455 slpm), the axial flow cyclone is able to remove particles below 100 nm efficiently, and the flow Reynolds number was found to have a great effect on the particle collection efficiency.

Keywords: Axial Flow cyclone; Air pollution control; Particle control

1. Introduction

A cyclone separator is a well-known dust separator or particle sampling device which is based on the particle centrifugal force created by vortex flow in the cyclone. There are two main designs: tangential and axial flow cyclones are the two main types. In a tangential flow cyclone, the flow enters tangentially in a cylinder creating a vortex inside. At the end of the outer vortex, the flow

* Corresponding author. Tel.: +886-3-5731880; fax: +886-3-5727835.
E-mail address: cjtsai@mail.nctu.edu.tw (C.-J. Tsai).

0021-8502/$ - see front matter © 2004 Elsevier Ltd. All rights reserved.
doi:10.1016/j.jaerosci.2004.03.007

Nomenclature

B	pitch of vanes
C	slip correction factor
d_p	particle diameter
d_{pa50}	cutoff aerodynamic diameter
e	charge of an electron
D	cyclone diameter (tangential flow cyclone)
D_e	exit tube diameter (tangential flow cyclone)
η	particle collection efficiency
Γ	a factor $= V/U_a$
I_c	electric current at the outlet of the cyclone
I_t	electric current at the outlet of the by-pass tube
k	number of charges
L	effective body length, distance from the tip of the outlet tube to the bottom of the spindle
λ	mean free path of air molecules at the inlet of the cyclone when pressure is P_{cyc}
λ_0	mean free path of air molecules at standard condition
N	number of vanes
n	number of vane turns
$n_c^o(d_{pk})$	particle concentrations at the outlet of the cyclone, the particle carries k charges
$n^i(d_{pk})$	inlet particle concentration, the particle carries k charges
$n_t^o(d_{pk})$	particle concentrations at the outlet of the by-pass tube, the particle carries k charges
Pen	overall penetration
P_{cyc}	pressure at the inlet of the cyclone
P_{760}	standard pressure, or 760 torr
$\mathrm{Pen}(d_{pk})$	particle penetration through the cyclone for a particle carries k charges
$\mathrm{Pen}_t(d_{pk})$	particle penetration through the by-pass tube for a particle carries k charges
Ψ_{50}	dimensionless cutoff aerodynamic diameter
Q	volumetric flow rate
Q_0	standard volumetric flow rate
r	new particle radial position
r_i	particle initial radial position
r_{max}	inner radius of the cyclone
r_{min}	radius of the vane spindle
Re'_f	flow Reynolds number (for tangential flow cyclone)
Re_f	flow Reynolds number (this study)
St	Stoke number defined as $St = \tau v_t/(r_{max} - r_{min})$
St_b	Stokes number defined in the body section, $St_b = \tau U_a/B$
t_v	particle transit time in the vane section
τ	particle relaxation time
U_a	mean axial gas velocity in the body section
U_i	inlet gas velocity (tangential flow cyclone)

v_r	particle radial velocity
v_t	tangential gas velocity in the vane section
V	mean gas velocity in the vane section
Vol	effective volume
w	vane thickness
ζ	a fitting constant

is reversed and finally exits axially at the top. The flow in the tangential cyclone is usually highly turbulent and non-stationary, which together with the flow reversal in the cyclone result in a relatively high pressure drop across the cyclone (in Maynard, 2000). The inlet and outlet of the tangential cyclone are perpendicular to each other. If the particle separator needs to be positioned in a straight section of a flow system, an axial flow cyclone may be used in which the tangential motion of the flow is induced by guiding vanes installed in line with the flow direction. The axial flow cyclone has a lower pressure drop than that of the tangential cyclone since the flow is in line with the axial direction of the cyclone, and the flow is not reversed and much less disturbed (Nieuwstadt & Dirkzwager, 1995).

Kao and Tsai (2001) reviewed many existing theories of the tangential flow cyclone including Lapple (1950), Stairmand (1951), Barth (1956), Leith and Licht (1972), Dietz (1981), Dirgo and Leith (1985), Iozia and Leith (1989), Li and Wang (1989), and Iozia and Leith (1990) and compared them with the existing data. They found that most theories are applicable in a certain range of flow Reynolds number only. The flow Reynolds number is based on the difference of the cyclone radius and that of the exit tube. At small flow Reynolds number, all theories under-predict the cutoff aerodynamic diameter and discrepancy increases as the flow Reynolds number is decreased.

Tsai, Shiau, Lin, and Shih (1999a, b) found that the cutoff aerodynamic diameter (the diameter corresponding to 50% penetration) of the 10 mm nylon cyclone to be lower than expected presumably due to build-up of deposited particles inside the cyclone. The nylon cyclone is for respirable particle collection. A similar cyclone with a bigger body diameter was developed, which was shown to have a less shift of the cutoff aerodynamic diameter and was also demonstrated to be more accurate in measuring respirable particle concentrations in the field study. Kenny, Gussman, and Meyer (2000) developed a sharp-cut tangential flow cyclone which was shown to have a sharp cut for ambient $PM_{2.5}$ sampling. The cutoff diameter of the cyclone was less affected by particle loading than the WINS (Well Impactor Ninety-Six) impactor (USEPA, 1997). In the laboratory dust loading study, Kenny et al. (2000) found WINS shifted steadily from 2.5 to 2.15 μm after sampling about 6 mg of $PM_{2.5}$ particles, while Peters and Vanderpool (1996) found a shift to 2.25 μm after sampling 24 mg of dust. The effect of deposited particles on the cutoff diameter was also studied earlier by Tsai and Cheng (1995) for impactors. Unless the body diameter is very small (such as 10 mm nylon cyclone), it is expected that the axial flow cyclones will be less affected by the loaded particles on the cutoff diameter than impactors since the particle deposit in the cyclones is more diffuse.

In contrast to the tangential flow cyclone, only few researchers have studied the axial flow cyclone, such as the experimental work of Liu and Rubow (1984), Weiss, Martinec, and Vitek (1987) and Vaughan (1988), and theoretical work of Maynard (2000). These researches studied the axial flow cyclone operating at ambient condition. For example, an axial flow cascade cyclone at

a design flow rate of 30 l/min was developed by Liu and Rubow (1984) for sampling high concentration of particles. The cutoff aerodynamic diameter of the five stages are 12.2, 7.9, 3.6, 2.05 and 1.05 μm. Total particle loss in the system, including the loss in the body, vane insert and exit tube of the collection cup, was shown to be significant. It ranged from 15% for particles of 1 μm in diameter to 33.3% for particles of 8 μm in diameter. Therefore, using this cascade cyclone to measure particle size distributions requires complete recovery of all particles lost in the cyclone.

Maynard (2000) derived the particle penetration of the axial flow cyclone based on the assumption that particle collection mainly occurs in the vane and body sections only. The overall penetration, Pen, is combined from the penetrations derived separately for the vane and body sections as

$$\mathrm{Pen} = (1-16\pi^2 St_b L^*)^{1/2} + \frac{4\pi^2 n^2 \Gamma^2 St_b^2}{r_{max}^{*2} - r_{min}^{*2}} - \frac{2n\Gamma St_b}{r_{max}^{*2} - r_{min}^{*2}} \left(1 + 4\pi^2 r_{min}^{*2} + 4\pi^2 \sqrt{1 - 16\pi^2 St_b L*}\right)^{1/2}, \tag{1}$$

where n is the number of vane turns, r_{max} is the inner radius of the cyclone, r_{min} is the radius of the vane spindle and L is the effective body length (refer to Fig. 1 in Maynard, 2000). The relative dimensions of these three variables, denoted by the variables with asterisk, is the actual dimension divided by the pitch of vanes, B. Stokes number St_b is defined in the body section as $St_b = \tau U_a/B$, in which τ is the particle relaxation time. The factor $\Gamma = V/U_a$, in which V is the mean gas velocity in the vane section and U_a is the mean axial gas velocity in the body section. If there are N vanes and each has a finite thickness w, then Γ in Eq. (1) is calculated as

$$\Gamma = \frac{r_{max}^* \sqrt{1 + 4\pi^2 r_{max}^{*2}}}{2(1 - Nw*)(r_{max}^* - r_{min}^*)}. \tag{2}$$

The form of Eq. (1) does not allow one to obtain a simple analytical form for St_{50} (Stokes number with 50% penetration), it must be calculated by numerical iteration.

In this study an axial flow cyclone operating at low pressure conditions (< 20 torrs) is designed and tested. The cyclone is expected to have submicron cutoff diameter and less particle bounce problems than impactors. In the following, first the theoretical collection efficiency and cutoff aerodynamic diameter of the axial flow cyclone is derived under low pressure condition. Then the experimental data obtained by using monodisperse oleic acid particles are used to validate the theoretical results. Finally, to match with the data, the need to adjust the cutoff aerodynamic diameter with the flow Reynolds number is demonstrated.

2. Theoretical method

In this study, the particle radial velocity and hence the collection efficiency is calculated theoretically based on the gas volumetric flow rate, properties of the cyclone, carrying gas and particles. The transit time of an aerosol particle in the vane section, t_v, is given by the ratio of the effective volume in the section (Vol) to the gas volumetric flow rate (Q). The effective volume in the vane, Vol, is

$$\mathrm{Vol} = \pi(r_{max}^2 - r_{min}^2)n(B - Nw), \tag{3}$$

where the other variables were described in the last section. Therefore the particle (or gas) transit time in the vane section, t_v, is

$$t_v = \frac{\pi(r_{max}^2 - r_{min}^2)n(B - Nw)}{Q}. \tag{4}$$

The tangential gas velocity in the vane section, v_t, can be calculated as

$$v_t = \frac{2\pi r_{min} nN}{t_v} = \frac{2r_{min} QN}{(r_{max}^2 - r_{min}^2)(B - Nw)} \tag{5}$$

Due to centrifugal force, $v_t^2\tau/r$, the particle will move in the radial direction. Neglecting the transient state of particle motion, the steady state particle radial velocity, v_r, is

$$v_r = \frac{dr}{dt} = \frac{\tau v_t^2}{r} = \frac{4\tau r_{min}^2 Q^2 N^2}{r(r_{max}^2 - r_{min}^2)^2(B - Nw)^2}. \tag{6}$$

Assuming that the particle (or the vortex) continues its spiral motion in the body section downstream of the vane such that it makes additional turns $n(\zeta - 1)$, where ζ is a fitting constant which gives the best agreement between the theoretical particle collection efficiencies and the published data in the literature. Adding the number of turns in the vane section, n, the total number of turns of the particle is $n\zeta$ in the cyclone. Rearranging Eq. (6) and integrating, the new particle radial position, r, at the end of spiral motion can be calculated based on the particle's initial radial position, r_i, at the inlet of the cyclone as

$$r^2 - r_i^2 = \frac{8\pi n\zeta\tau Q r_{min}^2 N^2}{(r_{max}^2 - r_{min}^2)(B - Nw)}. \tag{7}$$

Assuming plug flow and uniform particle concentration at the inlet of the cyclone, the particle collection efficiency (or $1 - \text{Pen}$), η, can be calculated as

$$\eta = \frac{r^2 - r_i^2}{r_{max}^2 - r_{min}^2} = \frac{8\pi n\zeta\tau Q r_{min}^2 N^2}{(r_{max}^2 - r_{min}^2)^2(B - Nw)} = 4\pi n\zeta St \frac{1}{1 + r_{max}/r_{min}}, \tag{8}$$

where St, the Stoke number, is defined as $St = \tau v_t/(r_{max} - r_{min})$. If $\zeta = 1$, Eq. (8) is similar to Eq. (12) in Maynard (2000) for calculation, the penetration through the vanes of the cyclone. Setting $\eta = 0.5$ in Eq. (8), the theoretical cutoff aerodynamic diameter, d_{pa50}, can be calculated as

$$d_{pa50} = \sqrt{\frac{9\mu(r_{max}^2 - r_{min}^2)^2(B - Nw)}{8\pi n\zeta Q r_{min}^2 N^2 C}}, \tag{9}$$

where the slip correction factor C is calculated as (Hinds, 1999)

$$C = 1 + \frac{\lambda}{d_p}\left[2.34 + 1.05\exp\left(-0.39\frac{d_p}{\lambda}\right)\right]. \tag{10}$$

At high vacuum, Eq. (10) is found to give the same friction coefficient as the molecular drag formula described in Rader and Geller (1998). Furthermore at high vacuum, C can be shown to be directly proportional to λ and indirectly proportional to d_p as

$$C = \frac{1.695\lambda}{d_p/2}. \tag{11}$$

This equation is accurate at high vacuum condition. For example, the difference in Eqs. (10) and (11) is less than 1% for particles smaller than 300 nm at 10 torr. Since the relationship between λ and the pressure at the inlet of the cyclone, P_{cyc}, at the isothermal condition is

$$\lambda = \frac{P_{760}\lambda_0}{P_{cyc}}, \tag{12}$$

then the slip correction factor can be re-written as

$$C = \frac{1.695 P_{760}\lambda_0}{P_{cyc} d_p/2}. \tag{13}$$

At a fixed standard flow rate Q_0, the actual flow rate $Q = Q_0\ (P_{760}/P_{cyc})$. Therefore, substituting Eq. (13) into Eq. (9), the cutoff aerodynamic diameter can be written as

$$d_{pa50} = 0.106 \left(\frac{P_{cyc}}{P_{760}}\right)^2 \frac{\mu(r_{max}^2 - r_{min}^2)^2(B - Nw)}{\rho_{po} n \zeta Q_0 r_{min}^2 N^2 \lambda_0}. \tag{14}$$

That is, at high vacuum, the cutoff aerodynamic diameter is proportional to the pressure at the inlet of the cyclone to the second power given that the standard flow rate is fixed.

However, at low pressure, the flow Reynolds number is usually very low and the cutoff aerodynamic diameter will be underestimated. For the tangential flow cyclone, Kao and Tsai (2001) found that the dimensionless cutoff aerodynamic diameter, Ψ_{50}, is a unique function of the flow Reynolds number, Re'_f, as follows:

$$\ln \Psi_{50} = -0.72 \ln Re'_f - 3.46, \tag{15}$$

where

$$\Psi_{50} = \frac{\sqrt{C} d_{pa50}}{D}, \tag{16}$$

$$Re'_f = \frac{\rho(D - D_e)U_i}{2\mu}, \tag{17}$$

where D and D_e are the cyclone and exit tube diameter, respectively. Similar correlation was found in Moore and McFarland (1996). It is expected that for the axial flow cyclone, the theoretical cutoff aerodynamic diameter, Eq. (9), has to be adjusted also by using the flow Reynolds number.

3. Experimental method

The experimental system is shown in Fig. 1. Monodisperse oleic acid particles of 35–460 nm ($\rho_p = 894\ kg/m^3$) were generated by the atomization and electrostatic classification technique. Oleic acid particles were first generated by atomizing 0.01 to 5% (v/v) oleic acid containing alcohol, dried by a silica gel drier, and finally classified by the TSI model 3080 electrostatic classifier with the TSI model 3081 long DMA. To obtain particles less than 100 nm, dried particles were further evaporated in a furnace and subsequently grown by condensation before electrostatic classification.

The axial flow cyclone was designed with $r_{max} = 1.5$ cm, $r_{min} = 1.0$ cm, $B = 0.5$ cm (design 1) or $B = 1.0$ cm (design 2). The effective cyclone body length (or the distance between the tip of the outlet tube and the bottom of the vane spindle), L, is 2.0 cm, and the inside diameter of the outlet

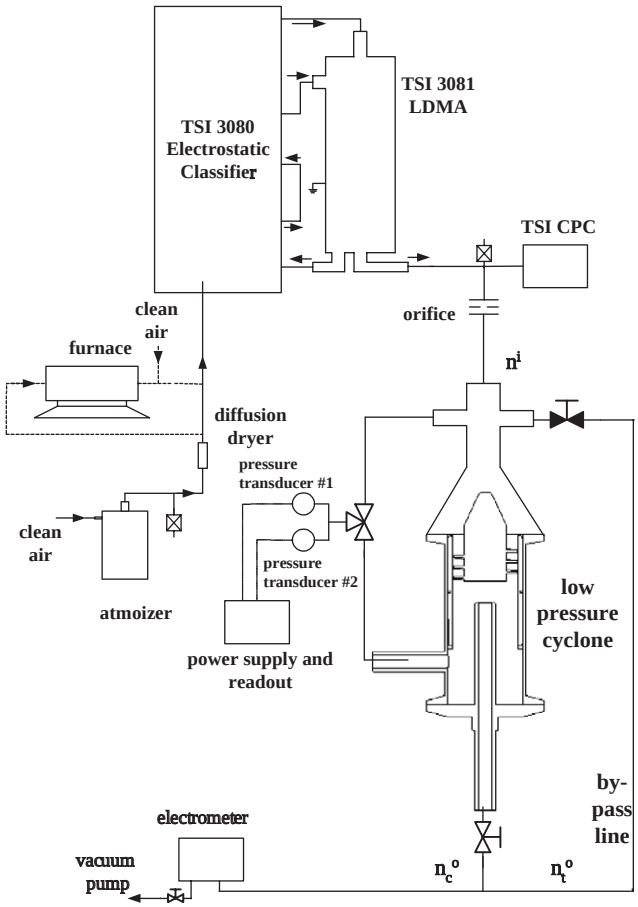

Fig. 1. Present experimental setup.

tube is 0.776 cm in this study. Two different vanes were designed as shown in Fig. 2. Design 1 has one vane which makes 3 complete turns; and design 2 has 3 vanes each makes half of a turn. Two different flow rates, 0.455 and 1.0 slpm were tested. Inlet cyclone pressure tested was 13, 14, 15, 16, 17 or 20 torr at 1 slpm, or 6, 8, 10, 13 torr at 0.455 slpm.

The steadiness of the concentration of classified monodisperse particles was monitored by the TSI model 3025A CPC (condensation particle counter) before the aerosol entered a critical orifice (O'Keefe Controls Co., V-14, 1 slpm; or V-9, 0.455 slpm). The TSI model 3068 electrometer or a home-made Faraday cage with the Keithley model 6514 electrometer was used to measure aerosol current after the cyclone, and after the by-pass tube for calculating the particle collection efficiency. The vacuum pump (SV16 10981, SOGEVAC, France, nominal pumping speed: 16 m^3/h) was used to create the flow and the pressure inside the cyclone was measured by the MKS Baratron type, 626A13TAE (1000 torr max.) or MKS Baratron type, 626A11TAE (10 torr max.)

Since the collection efficiency is determined by current measurement, the penetration of a singly charged particle with the diameter of d_{p1} will be influenced by the penetration of particles with k multiple charges (diameter d_{pk}), especially for particles greater than 100 nm. The electric currents,

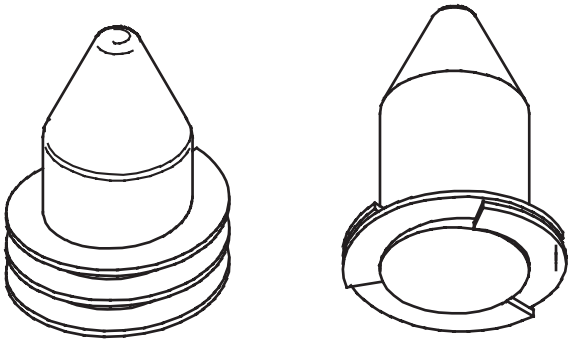

Fig. 2. Vanes of design 1 and 2.

I_c and I_t, were measured at the outlet of the cyclone and by-pass tube, respectively. The currents are related to flow rate Q, and inlet particle concentration $n^i(d_p)$ as

$$I_c = Qe\left(\sum_{k=1}^{\infty} kn^i(d_{pk})\mathrm{Pen}(d_{pk})\right), \tag{18}$$

$$I_t = Qe\left(\sum_{k=1}^{\infty} k\,n^i(d_{pk})\mathrm{Pen}_t(d_{pk})\right), \tag{19}$$

where k is the number of charges, e is the elementary charge. The particle penetration of the cyclone, $\mathrm{Pen}(d_p)$, and the particle penetration through the by-pass tube, $\mathrm{Pen}_t(d_p)$, are defined as

$$\mathrm{Pen}(d_p) = n_c^o(d_p)/n^i(d_p), \tag{20}$$

$$\mathrm{Pen}_t(d_p) = n_t^o(d_p)/n^i(d_p), \tag{21}$$

where $n_c^o(d_p)$ and $n_t^o(d_p)$ are particle concentrations at the outlet of the cyclone and by-pass tube, respectively.

It can be shown by simple algebraic manipulation of Eqs. (18)–(21) that Pen (d_{p1}) is

$$\mathrm{Pen}(d_{p1}) = \frac{I_c}{I_t}\left(\mathrm{Pen}_t(d_{p1}) + \sum_{k=2}^{\infty}\frac{kn^i(d_{pk})\mathrm{Pen}_t(d_{pk})}{n^i(d_{p1})}\right) - \sum_{k=2}^{\infty}\frac{kn^i(d_{pk})\mathrm{Pen}(d_{pk})}{n^i(d_{p1})}. \tag{22}$$

In this study, $\mathrm{Pen}_t(d_{pk})$ was found to be close to that of the cyclone without vanes. Therefore $\mathrm{Pen}_t(d_{pk})$ was assumed to be 1.0. The above equation was used to correct for multiple charge effect on the penetration of a single charge particle with diameter d_{p1}. When using Eq. (22), one normally has to measure the penetration of the largest particles first, which is determined by the cutoff diameter of the impactor at the DMA inlet. This penetration is known to be accurate since there is no multiple charge effect for the largest particles entering DMA. Then the penetration of smaller particles is measured and corrected for the multiple charge effect by Eq. (22).

4. Results and discussion

The theoretical cutoff aerodynamic diameter of the present study is first compared with the previous experimental data in the literature. As shown in Fig. 3, at 1 atm the theoretical cutoff aerodynamic diameters, Eq. (9), compare very well with the previous experimental data of Liu and Rubow (1984) (symbol: circle), Weiss et al. (1987) (symbol: square), and Vaughan (1988) (symbol: triangle). One exception is the experimental data point near 4.8 μm which has a large deviation from the present prediction. The experimental cutoff aerodynamic diameter ranges from 1.05 to 12.2 μm. It was found that best agreement was obtained if the number of turns in the cylindrical body after the vane was assumed to be half of the number of vane turns. That is, ζ was assumed to be 1.5 in Eq. (9).

The theoretical prediction by Maynard (2000), Eq. (1), also gives similar agreement, with larger deviation for some data points of large particles.

The pressure at the inlet (before the vane) and outlet (after the vane) of the cyclone were measured and shown in Fig. 4. Design 1 with one 3-turn vane has higher pressure drop than design 2 with 3 half turn vanes, due to lower air flow velocity in the vane in the latter compared to that in the former. At 1 slpm, the lowest pressure achieved is 13 torr at the cyclone inlet, and the pressure drop (inlet pressure minus outlet pressure) is 4 and 2.9 torr for design 1 and 2, respectively. The pressure drop decreases with an increasing inlet pressure. At the inlet pressure of 23 torr, the pressure drop becomes 1.8 and 1.4 torr for design 1 and 2, respectively. Higher vacuum is achieved at lower volumetric flow rate. At 0.455 slpm, the highest vacuum achieved is 6 torr at the cyclone inlet, and the pressure drop for design 1 and 2 is 3.3 and 2.32 torr, respectively. The pressure at the stagnation

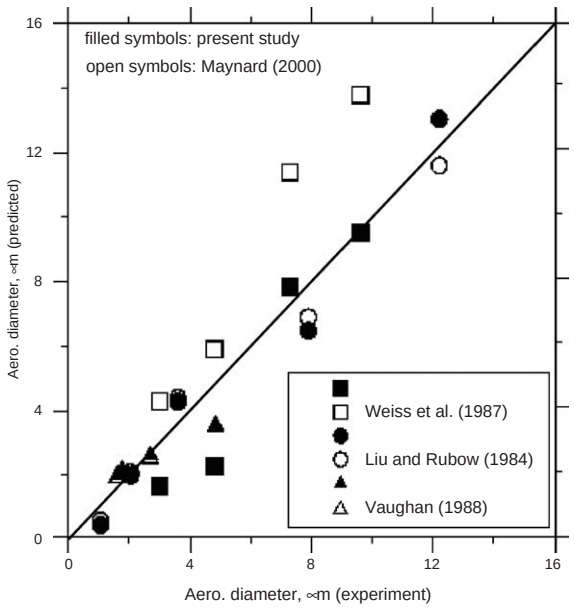

Fig. 3. Comparing the cutoff aerodynamic diameter of the present theory with previous experimental data.

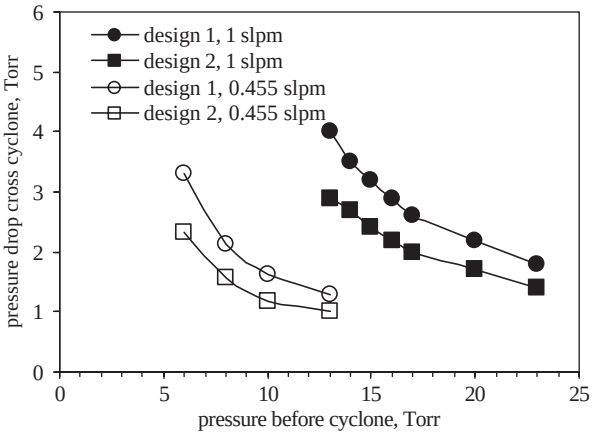

Fig. 4. Pressure in the cyclone.

point should be used to calculate the efficiency (Biswas & Flagan, 1984). As this cannot be readily obtained, in this study, the average of the inlet and outlet pressure was used to calculate particle collection efficiency.

The experimental particle collection efficiency curves are shown in Figs. 5(a)–(d) for two flow rates and two vane designs. In general, a lower pressure results in a higher particle collection efficiency, and design 1 has higher collection efficiency than design 2. For design 1, at the flow rate of 0.455 slpm and the inlet pressure of 6 torr, the collection efficiency increases from 32% to nearly 100%, as the particle diameter of oleic acid is increased from 35 to 100 nm (Fig. 5(a)). The cutoff diameter is 48.7 μm. As the inlet pressure is increased from 6 to 8, 10 or 13 torr, the collection efficiency drops considerably and the curves look less like S-shaped. The cutoff diameter is increased to 153.4 and 330 nm for the inlet pressure of 8 and 10 torr, respectively.

For design 2, at the same flow rate of 0.455 slpm, and the same inlet pressure as design 1, the corresponding collection efficiency is lower (Fig. 5(b)). Lower pressure drop of design 2 is mainly responsible for the lower particle collection efficiency, which agrees with the observation of traditional cyclones. The cutoff diameter of design 2 is much larger than design 1, which is 107.6 and 343.2 nm for the inlet pressure of 6 and 8 torr, respectively.

As the flow rate is increased to 1 slpm, the minimum inlet pressure, 13 torr, is higher than that of 0.455 slpm. The particle collection efficiency curves shown in Figs. 5(c) and (d) follow the similar trend as in the previous figures. That is at the same inlet pressure, design 1 has higher collection efficiency than design 2, and inlet pressure has a very important effect on particle collection efficiency. When the inlet pressure is increased from 13 to 20 torr, the cutoff diameter increases from 120.5 to 411 nm for design 1, and from 145.5 to 600 nm for design 2.

When compared to the present theory, Eqs. (8) and (9), it is found that experimental collection efficiency is much lower, and the experimental cutoff aerodynamic diameter is much larger for all particle diameters. This is due to the Reynolds number effect (Kao & Tsai, 2001; Moore & McFarland, 1993) as pointed out in the previous section. Thus, the cutoff aerodynamic diameter has to be correlated with the flow Reynolds number, in a form similar to the right-hand side of Eq. (15)

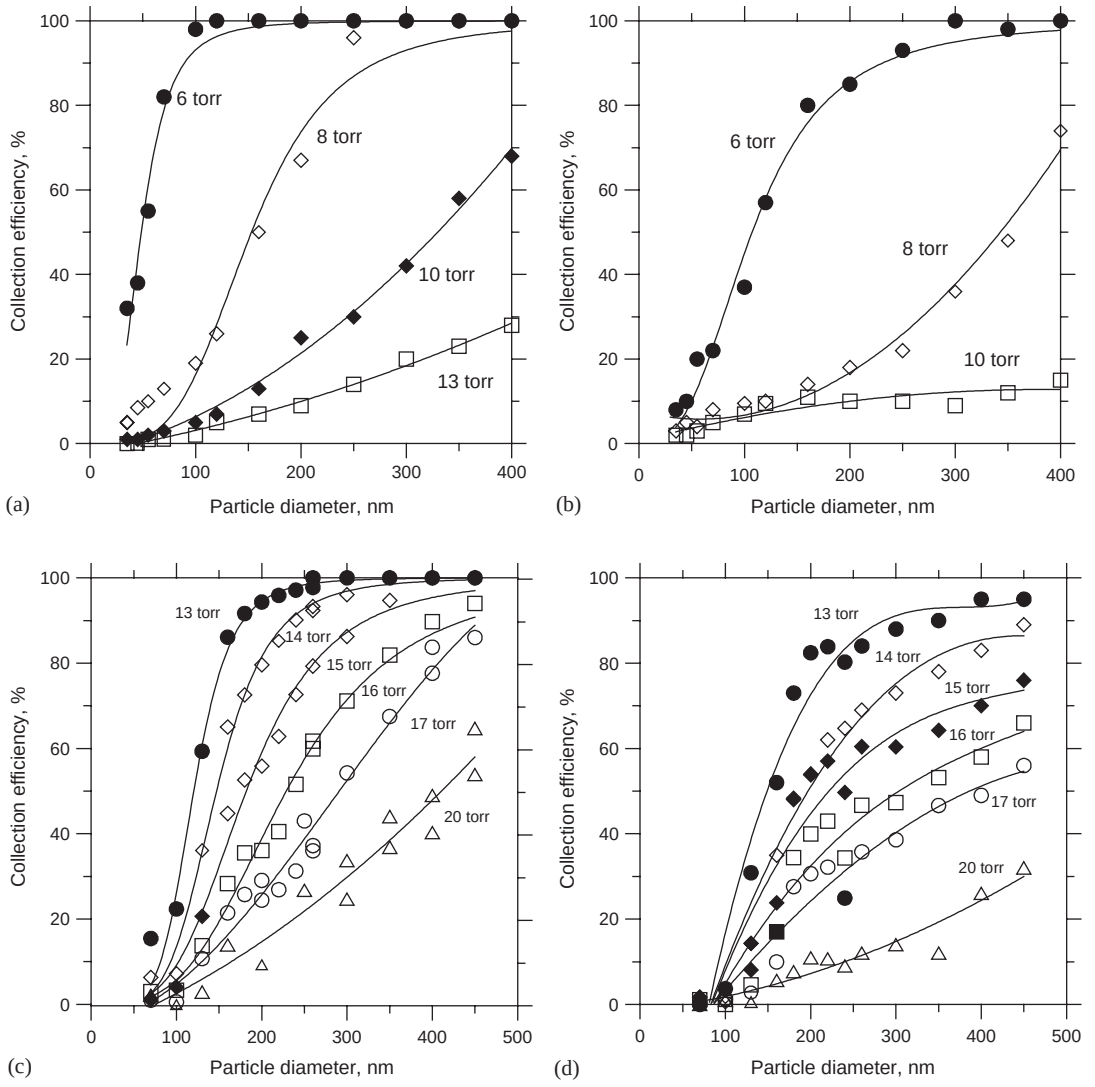

Fig. 5. Particle collection efficiency versus particle diameter (a) $Q = 0.455$ slpm, design 1; (b) $Q = 0.455$ slpm, design 2; (c) $Q = 1$ slpm, design 1; (d) $Q = 1$ slpm, design 2.

but with different empirical constants. It is found that the following cutoff aerodynamic diameter, d_{pa50}, adjusted empirically from Eq. (9) by the flow Reynolds number gives good agreement with the experimental data:

$$d_{\mathrm{pa50}} = \sqrt{\frac{9\mu(r_{\max}^2 - r_{\min}^2)^2(B - Nw)}{8\pi n\zeta Q r_{\min}^2 N^2 C}} \times \exp(-0.276\ln(Re_{\mathrm{f}}) + 1.18), \tag{23}$$

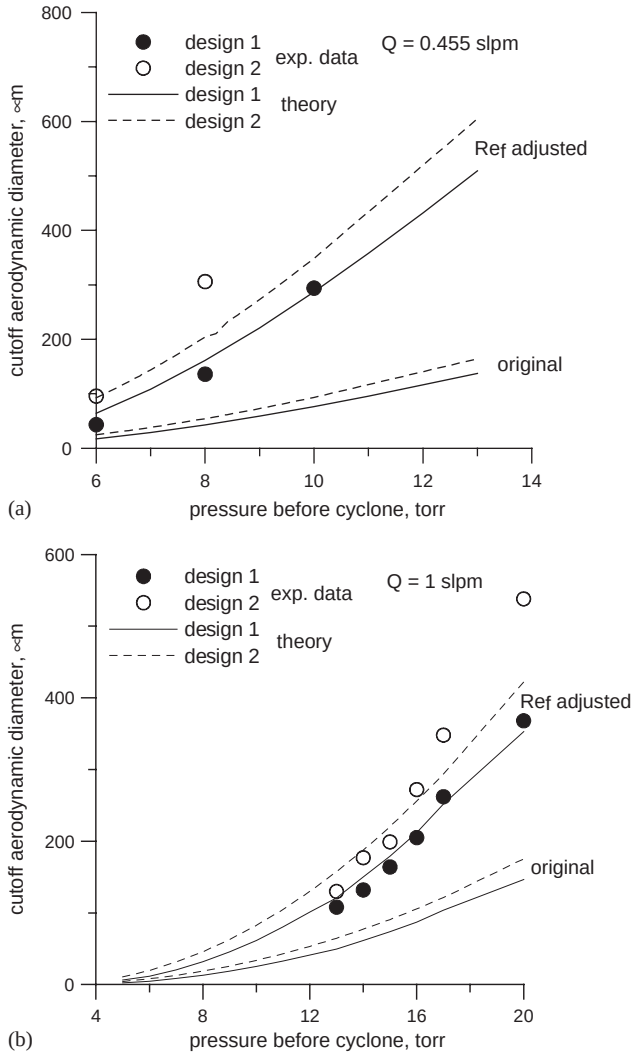

Fig. 6. Comparison of theoretical cutoff aerodynamic diameter with experimental data. (a) $Q=0.455$ slpm; (b) $Q=1$ slpm.

where the flow Reynolds number is now defined as

$$Re_{\mathrm{f}} = \frac{\rho(r_{\max} - r_{\min})U_{\mathrm{a}}}{\mu} \tag{24}$$

and U_{a} is the average axial velocity through the cyclone vane.

Fig. 6 shows the comparison of theoretical cutoff aerodynamic diameter with the experimental data. As can be seen, the original theory, Eq. (9), underestimates the cutoff aerodynamic diameter substantially at low flow Reynolds number of $Re_{\mathrm{f}} = 6.4$ for 0.455 slpm, and $Re_{\mathrm{f}} = 14.1$ for 1 slpm. At $Re_{\mathrm{f}} = 6.4$ and 14.1, the experimental cutoff aerodynamic diameters are 2.7 and 3.4 times the theoretical values. After correlating with the flow Reynolds number, it is found that Eq. (23) is

able to predict the cutoff aerodynamic diameter at different inlet pressures, flow rates and cyclone designs.

5. Conclusions

An axial flow cyclone with an inner diameter of 3.0 cm was designed and tested to remove fine particles at low pressure (6–23 torr) and low flow rate (0.455 and 1.0 slpm) conditions. Pressure inside the cyclone was found to have a considerable effect on the particle collection efficiency. At lower pressure, the particle collection efficiency was also found to be higher. The cyclone with higher pressure drop has higher collection efficiency. At a fixed inlet pressure, higher pressure drop of design 1 with one 3-turn vane was found to have a higher collection efficiency than design 2 with three half-turn vanes. At lowest achievable pressure of 6 torr at the flow rate of 0.455 slpm in this study, the axial flow cyclone of design 2 is able to remove particles below 100 nm efficiently, and the cutoff aerodynamic diameter is 43.3 nm.

Theoretical prediction of cutoff aerodynamic diameter was found to agree with published experimental data in the literature at ambient conditions. However, at vacuum and low flow rate conditions, experimental collection efficiency was found to be much lower than theoretical efficiency. Based on the experimental data, a semi-empirical equation incorporating the flow Reynolds number was developed to predict the cutoff aerodynamic diameter with good accuracy at different inlet pressures, flow rates and cyclone designs.

This low flow rate axial flow cyclone is applicable for fine particle removal in the low pressure exhaust gas of reaction chambers, such as in the semiconductor and optoelectronic industries. In the future, it is worthwhile to study the effect of particle loading in the cyclone and particle material on the particle collection efficiency.

Acknowledgements

Authors would like to thank for the financial support of this project by the Industrial Technology Research Institute (ITRI) in Taiwan in 2003, and Taiwan National Science Council (NSC 92-2211-E-009-016).

References

Barth, W. (1956). Design and layout of cyclone separator on the basis of new investigations. *Brennst Warme Kraft*, *8*, 1–9.

Biswas, P., & Flagan, R. C. (1984). High-velocity inertial impactors. *Environmental Science and Technology*, *18*, 611–616.

Dietz, P. W. (1981). Collection efficiency of cyclone separtors. *A.I.Ch.E. Journal*, *27*, 888–892.

Dirgo, J., & Leith, D. (1985). Cyclone collection efficiency: Comparison of experimental results with theoretical predictions. *Aerosol Science and Technology*, *4*, 401–415.

Hinds, W. C. (1999). *Aerosol technology* (2nd ed.) (p. 127). New York: Wiley.

Iozia, D. L., & Leith, D. (1989). Effect of cyclone dimensions on gas flow pattern and collection efficiency. *Aerosol Science and Technology*, *10*, 491–500.

Iozia, D. L., & Leith, D. (1990). The logistic function and cyclone fractional efficiency. *Aerosol Science and Technology*, *12*, 598–606.

Kao, K. Y., & Tsai, C. J. (2001). On the theory of particle collection efficiency of cyclones. *Journal of Aerosol and Air Quality*, *1*, 47–56.

Kenny, L. C., Gussman, R., & Meyer, M. (2000). Development of a sharp-cut cyclone for ambient aerosol monitoring applications. *Aerosol Science and Technology*, *32*, 338–358.

Lapple, C. E. (1950). Gravity and centrifugal separation. *Industrial Hygiene Quarterly*, *11*, 40–48.

Leith, D., & Licht, W. (1972). The collection efficiency of cyclone type particle collectors: a new theoretical approach. *A.I.Ch.E. Symposium Series*, *126*, 196–206.

Li, E., & Wang, Y. (1989). A new collection theory of cyclone separators. *A.I.Ch.E. Journal*, *35*, 666–669.

Liu, B. Y. H., & Rubow, K. L. (1984). A new axial flow cascade cyclone for size characterization of airborne particulate matter. In: Liu, B. Y. H., Pui, D. Y., & Fissan, H. J. (Eds.), *Aerosols* (pp. 115–118). Amsterdam: Elsevier.

Maynard, A. D. (2000). A simple mode of axial flow cyclone performance under laminar flow conditions. *Journal of Aerosol Science*, *31*, 156–167.

Moore, M. E., & McFarland, A. R. (1993). Performance modeling of single-inlet aerosol sampling cyclone. *Environmental Science and Technology*, *27*, 1842–1848.

Moore, M. E., & McFarland, A. R. (1996). Design methodology for multiple inlet cyclones. *Environmental Science and Technology*, *30*, 271–276.

Nieuwstadt, F. T. M., & Dirkzwager, M. (1995). A fluid mechanics model for an axial cyclone separator. *Industrial Engineering and Chemical Research*, *34*, 3399–3404.

Peters, T. M., & Vanderpool, R. W. (1996). Modification and evaluation of the WINS impactor. R. T. I. Report No. 6360-011.

Rader, D. J., & Geller, A. S. (1998). Showerhead-enhanced inertial particle deposition in parallel-plate reactors. *Aerosol Science and Technology*, *28*, 105–132.

Tsai, C. J., & Cheng, Y. H. (1995). Solid particle collection characteristics on impaction surfaces of different designs. *Aerosol Science and Technology*, *23*, 96–106.

Tsai, C. J., Shiau, H. G., Lin, K. C., & Shih, T. S. (1999a). Effect of deposited particles and particle charge on the penetration of small sampling cyclones. *Journal of Aerosol Science*, *30*, 313–323.

Tsai, C. J., Shiau, H. G., & Shih, T. S. (1999b). Field study of the accuracy of two respirable sampling cyclones. *Aerosol Science and Technology*, *31*, 463–472.

USEPA, 1997, *Ambient Air Monitoring Reference and Equivalent Methods*. United States Environmental Protection Agency, Federal Register 40 CFR Parts 50.

Vaughan, N. P. (1988). Construction and testing of an axial flow cyclone pre-separator. *Journal of Aerosol Science*, *19*(3), 295–305.

Weiss, Z., Martinec, P., & Vitek, J. (1987). *Vlastnosti Dulnibo Prachu A Zaklady Protiprasne Techniky*. SNTL: Prague.